

Shrinkage of Mt. Bogda Glaciers of Eastern Tian Shan in Central Asia during 1962–2006

Kaiming Li^{*1}, Zhongqin Li^{1,2}, Cuiyun Wang¹, Baojuan Huai²

1. School of Architecture and Urban Planning, Lanzhou City University, Lanzhou 730070, China

2. Cold and Arid Region Environmental and Engineering Research Institute, Chinese Academy of Sciences, Lanzhou 730000, China

ABSTRACT: Many small mountain glaciers have been reported undergoing strong shrinkage, and it is therefore important to understand how they respond to climate change. The availability of topographic maps from 1962, Landsat TM imagery from 1990 and ASTER (Advanced Spaceborne Thermal Emission and Radiometer) imagery from 2006 and field investigation of some glaciers allow a comprehensive analysis of glacier change based on glacier size and topography on Mt. Bogda. Results include: (1) an overall loss of a glacierized area by $31.18 \pm 0.31 \text{ km}^2$ or 21.6% from 1962 to 2006, (2) a marked dependence of glacier area shrinkage on initial size, with smaller glaciers experiencing higher shrinkage levels, (3) the disappearance of 12 small glaciers, (4) a striking difference in area loss between the southern and northern slopes of 25% and 17%, respectively. A subset of the investigated glaciers shows that the area $57.45 \pm 0.73 \text{ km}^2$ in 1962 reduced to $54.79 \pm 0.561 \text{ km}^2$ in 1990 and $48.88 \pm 0.49 \text{ km}^2$ in 2006, with a relative area reduction of 4.6% during 1962–1990, and 10.8% during 1990–2006. The corresponding volume waste increased from 6.9% to 10.2%. Three reference glaciers were investigated in 1981 and revisited in 2009. Their terminus experienced a marked recession. Meteorological data from stations around Mt. Bogda reveals that glacier shrinkage is correlated with winter warming and an extension of the ablation period. Precipitation on the northwest side of the range shows a marked increase, with a slight increase on the southeast side.

KEY WORDS: glacier shrinkage, climate change, water resources, Bogda Mountain, Tian Shan.

0 INTRODUCTION

The cryosphere, to the global hydrological cycle, is composed of snow cover, glacier and ice in different forms. About 10% of the Earth's land surface is permanently covered by glaciers. The melted glacier water supplies the runoffs during warm days, and is also a reliable water source during droughts. However, the available fresh water stored in alpine glaciers is gradually decreasing and changing the cryosphere regime because global warming is causing increased glacier melting. Many mountain ranges have undergone a decrease in the rate of glacierization due to ongoing climate changes, and secular mass loss has been considered a worldwide phenomenon for the past several decades (WGMS, 2008).

Glaciers in the Tian Shan Mountains, as well as catchments in alpine regions, are of considerable importance as water resources, especially in the arid and semi-arid Xinjiang region in China (Li et al., 2011a). In the context of water availability, it is necessary to understand its past fluctuations, current states and future evolution as atmospheric warming is predicted to continue (Cubasch and Meehl, 2001).

Glacier changes in the Tian Shan Mountains have received

extensive attention in recent years due to concern of water shortage. There is continued interest in mapping glaciers using satellite data (Narama et al., 2010; Kutuzov and Shahgedanova, 2009; Aizen et al., 2007; Bolch, 2007; Niederer et al., 2007) or field observations on the Urumqi Glacier No. 1 (UG1) in China (Li et al., 2007, 2003). The majority of assessments regarding glacier changes focused on Tian Shan in a range of 67°E–80°E, while very little research has been done on eastern Tian Shan with a large range between 80°E–95°E (Table 1). Particularly important is the fact that mountainous areas provide water for the extremely water-stressed Turfan Basin (Fang et al., 2010), which is why the glacier changes of Mt. Bogda need to be investigated further to understand the relationship between glacier and climate change.

Marked regional differences of the glacier's relative area change exist in well-investigated regions (Narama et al., 2010). This is also embodied in Table 1 with a rate of -3.3%– -32% in a different time span. Though the results may be partly affected by the available data sources and investigated sample size, the ice mass loss is beyond doubt.

1 STUDY AREA

The study area is in the western section of Mt. Bogda (43°10'N–44°5'N, 87°40'E–91°35'E), the largest glacierized area in eastern Tian Shan, which is located 90 km east of Urumqi City in the Xinjiang Uygur Autonomous Region of China (Fig. 1). The range is 330 km long, stretching from east to west with an area of 20 000 km². Condensed on the Bog-

*Corresponding author: lkm_wd@126.com

© China University of Geosciences and Springer-Verlag Berlin Heidelberg 2016

Manuscript received June 19, 2014.

Manuscript accepted January 28, 2015.

da-Peak (5 445 m a.s.l.) are several of eastern Tian Shan's largest glaciers. Based on the Glacier Inventory of China (III) (Wang et al., 1986), which is also a part a World Glacier Inventory (WGI) (http://nsidc.org/data/glacier_inventory/), there were 469 glaciers in the mountain with a total area of approximately 214 km² in the 1960s, ranging from 0.02 to 10.27 km² with a mean size of 0.46 km². One of the typical characteristics of Mt. Bogda is the asymmetry of northern and southern slopes.

The southern slope is less steep with a long bank compared to the northern slope. The typical topography provides more high land for snow accumulation and thus is favorable for glacier development. According to Wang et al. (1986), there were 256 glaciers covering 122.35 km² in the southern slope and 213 glaciers in the northern slope covering 91.50 km².

The Bogda Mountain is poorly controlled by the westerly air mass and the influence of Siberian anticyclonic circulation,

Table 1 Glacier area change in Tian Shan Mountains during the past several decades

Region	Location	Data sources	Period	Area loss (%)	Reference
67°E–80°E					
Pskem	42°N, 71°E	Corona/ Landsat ETM+ / ALOS	1970–2000	19	Narama et al., 2010
			2000–2007	5	
Ala Archa	42°N, 74°E	ASTER	1963–1981	5.1	Aizen et al., 2007
			1963–2003	15.7	
Sokoluk	42°N, 74°E	Landsat ETM	1963–2000	28	Niederer et al., 2007
Terskey-Alatoo	42°N, 74°E	Landsat TM/ ASTER	1965–2003	12.6	Kutuzov and Shahgedanova, 2009
			1990–2003	3.8	
At-Bashy	41°N, 75°E	Corona/ Landsat ETM+ / ALOS	1970–2000	12	Narama et al., 2010
			2000–2007	4	
Ak-shirak	43°N, 75°E	ASTER	1943–2001	26	Khromova et al., 2003
SE-Fergana	41°N, 76°E	Corona/ Landsat ETM+ / ALOS	1970–2000	9	Narama et al., 2010
			2000–2007	0	
Terskey Alatoo	42°N, 77°E	Corona/Landsat ETM+	1971–2002	8	Narama et al., 2006
Ili-Kungoy	43°N, 77°E	Corona/ Landsat ETM+ / ALOS	1970–2000	12	Narama et al., 2010
			2000–2007	4	
Akshirak	42°N, 78°E	ASTER	1943–1977	4.2	Aizen et al., 2007
			1943–2003	12.8	
Zailiyskiy and Kungey Alatau	43°N, 75°E–79°E	Landsat ETM	1955–1999	32	Bolch, 2007
80°E–95°E					
Akesu	42°N, 80°E	Landsat TM/ETM+	1963–1999	3.3	Liu et al., 2006
Kaidu River	42°N, 85°E	Landsat ETM+/ SPOT1	1963–2000	13	Li et al., 2006
Urumqi River	43°N, 86°E	Aerial photogrammetry	1964–1992	13.8	Chen et al., 1996
UG1	43°06'N, 85°49'E	Field measurement	1962–2000	11	Li et al., 2007, 2003
			1962–2006	14	
Karlik Shan	43°N, 94°E	Landsat TM/ ETM+/ ASTER	1971–2002	5.3	Wang et al., 2009

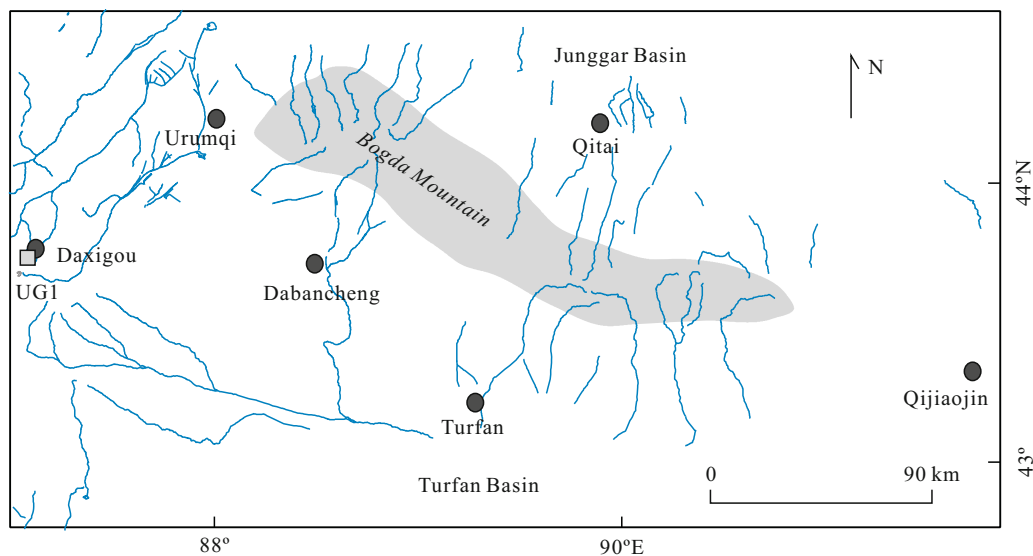


Figure 1. Sketch map showing the study area on Mt. Bogda.

where precipitation mainly occurs in summer, with cold and dry weather in winter (Aizen et al., 1997). Large-scale simulations reflect spatial and seasonal variations in central and high Asia (Böhner, 2006). The Bogda Range is largely affected by local convective processes. Precipitation varies horizontally. Qitai (794 m a.s.l.) on the south and Urumqi (935 m a.s.l.) on the west are <300 mm. Dabancheng (1 104 m a.s.l.) and Turfan (345 m a.s.l.) on the south are <50 mm. Qijiaojin (721 m a.s.l.) on the east is 35 mm. However, the precipitation at Daxigou Station, with an altitude of 3 539 m a.s.l., is 450 mm (Fig. 2). Generally, the minimum precipitation occurs in winter, and the summer maximum is even more pronounced at all sites.

The range is likely posing a barrier to prevent air masses from northwest and west from passing through. The southern slopes turned into rain shadow with little precipitation (Wu et al., 1983a). The 0 °C isothermal line of the southern and northern slope is situated around 2 800 and 2 500 m a.s.l., respectively (Wang and Qiu, 1983). Precipitation reaches 670 mm above 4 000 m a.s.l. on the southern slope and above 3 900 m a.s.l. on the northern slope, respectively (Wu et al., 1983a). Due to topographic effects, climatic settings of the Turfan Basin in the southern side tend to be fairly arid, while the Junggar Basin in the northern side is relatively humid. The maximal mean annual air temperature (MAAT) is 14.4 °C in Turfan and only 5.2 °C in Qitai (Fig. 2).

Although great differences of air temperature and precipitation are found in the low and middle regions between the northern and southern slopes, it has been pointed out that the annual rainfall is about 700–750 mm at the elevation of 4 100 m a.s.l., and the precipitation concentrates in summer in this region according to the field investigation during 1985–1986 (Wang et al., 1989). It is suggested that the precipitation in the Alpine region in the southern slope is close to that in the northern slope.

2 DATA AND METHODS

2.1 Data Sources

The historical information of the glacier range was acquired from six 1 : 50 000 scale topographic maps, which were based on 1962 aerial photographs. Those maps were printed in 1973 by the Bureau of Surveying and Mapping of the Chinese

People's Liberation Army. The topographic maps were first scanned at 600 dpi and then digitized to produce DEM with a resolution of 25 m. The ground resolution of the maps is approximately 5 m. The error in measuring glacier area on topographic maps and aerial photography is estimated to be less than 5% (Wang et al., 1986).

The recent glacial coverage depends mainly on the delineation of the glaciers from Landsat TM with a spatial resolution of 30 m acquired on 9/10/1990 and Advanced Spaceborne Thermal Emission and Radiometer (ASTER) imagery (ASTLIB) with a ground resolution of 15 m acquired on 21/09/2006. The selected scenes were all obtained under cloud-free conditions for immunity of potential error and for the ablation period, when the extent of snow-cover is minimal to reject the perturbation in delineating the glacier outlines. The field investigation confirmed that debris cover is not extensive in this region and most of the glacier surface is clean. It is helpful to improve the accuracy of the mapped glacier area.

2.2 Glacier Mapping

To enable a direct comparison and to quantify the glacier changes, all glacier boundaries in topographic maps were digitized from the scanned maps. The extent of each glacier from satellite scenes was mapped manually on-screen under the support of ArcGIS 9.2. Glacier length was determined by manually digitizing hypothetical flowlines. Digitization starts at the lowest point of a glacier and follows a central flowline until the highest point is reached. The line crosses the contour lines perpendicularly (Svoboda and Paul, 2009). Glacier outline in 1962 topographic map was set as the benchmark. All later lines of the glacier were measured in order to be consistent with earlier mapping. All work was done by one person, as this is important to keep the records consistent for manual delineation (Bolch et al., 2008; WGMS, 2008). To the split glacier, the area from imagery was integrated based on the individual fragments.

Glacier parameters (area, length, elevation, etc.) and glacier mapping were attained under the Global Land Ice Measurements from Space (GLIMS) workshop (Racoviteanu et al., 2009; Raup et al., 2007a, b). Data assessments conducted have confirmed that artificial interpretation remains an effective tool

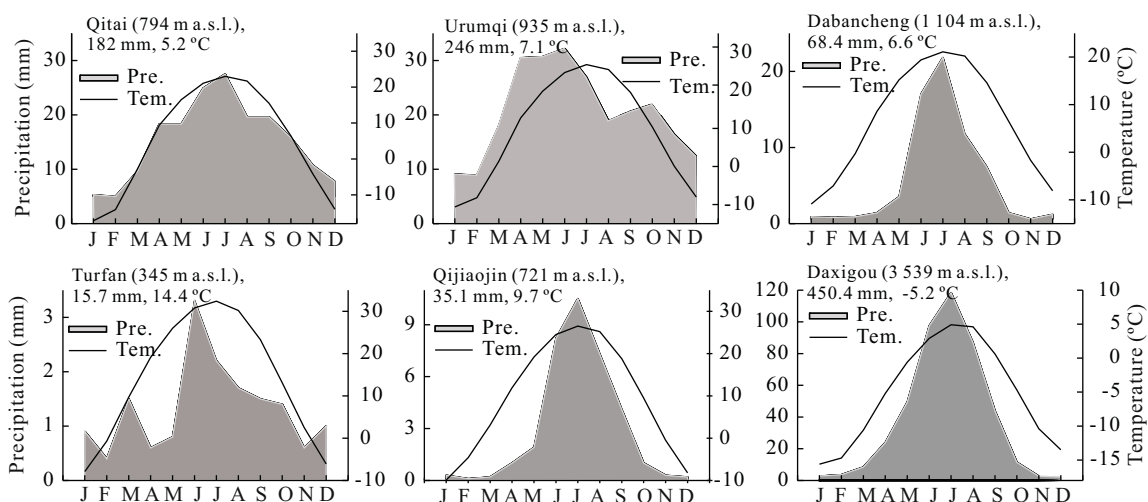


Figure 2. Diagrams showing precipitation and temperature information of six meteorological stations during 1959–2002. Their locations in Fig. 1.

for extracting higher level information from satellite imagery for glaciers (Raup et al., 2007a), especially when glaciers are covered by debris or mapping in the accumulation zone (Bolch et al., 2010, 2008; Raup et al., 2007b). The GIS-based processing of classified glacier maps and ASTER images including parameters extraction and calculation were conducted under the previous method and theory (Paul and Andreassen, 2009; Svoboda and Paul, 2009; Kääb et al., 2002).

The imagery covered the part of Bogda Mountain and thus it includes only 191 glaciers, not all 469 glaciers. Some glaciers around Bogda-Peak were field investigated by the Chinese and Japanese expeditions in the summer of 1981. The expeditions provide information of glacial terminus variations (Wang and Qiu, 1983; Wu et al., 1983a, b). This systematic survey also provides the physics and chemical characteristic description of investigated glaciers and analysis of regional climate conditions (e.g., Xie et al., 1983).

Glacier volume and change estimation using the scaling method are only dependent on planar information (Bahr et al., 2009, 1997; Liu et al., 2003). However, the approach by Haeberli and Hoelzle (1995) and Driedger and Kennard (1986), which is based on the glacier surface inclination and elevation range could be used to estimate the volume in combination with thickness and area. The glacier aspect and elevation in 1962, 1990 and 2006 were acquired based on the DEM. The average thickness (h_F) of the entire glacier is estimated to be $h_F=(\pi/4)h_f$. Here, the average ice depth along the central flowline h_f is expressed as such: $h_f=\tau_f/f\rho g\cdot\sin\alpha$. Where τ_f is mean basal shear stress along the central flowline and is a function of mass turnover determined by the vertical extent, ρ is density, g is acceleration due to gravity, α is average surface slope, and f is shape factor and is chosen as 0.8 for all glaciers (Haeberli and Hoelzle, 1995). Thus, the total glacier volume V is equal to the total surface area A multiplied by the average thickness h_F and expressed as $V=A\cdot h_F$.

The corresponding thickness and volume estimates for individual glacier were calculated three-dimensionally rather than using the planar method. Further analysis could be taken by reconstructing the bedrock topography for glaciers (Linsbauer et al., 2009) and the parabolic shape of glacier beds without explicitly considering mass fluxes (Farinotti et al., 2009). Here, the thickness and volume were calculated depending on the approach introduced by Haeberli and Hoelzle (1995), which had been especially developed on behalf of the UNEP for the analysis of detailed glacier inventories.

2.3 Error Estimation

To co-register the images onto topographic maps, the scenes had to be orthorectified. The Landsat TM and ASTER imagery were orthorectified using ERDAS imagine software.

Twenty-four ground control points (GCPs) were taken from the map and the horizontal root-mean-square error (RMSE_{x,y}) with respect to GCPs was limited below 1 pixels. The projective transformation was performed based on those GCPs and the DEM produced from the digitized topographic maps. The DEM was not only used for the orthorectification but also for the glacier parameters extraction.

According to Wang et al. (1986), the uncertainty of glacier area on topographic maps and aerial photography was estimated to be less than 5%. Therefore the total uncertainty of the glacier area (U) in 1962 can be calculated based on the formula as follow (Wang et al., 2009; Jin et al., 2005)

$$U = \sqrt{(A_1 \times 5\%)^2 + (A_2 \times 5\%)^2 + \dots + (A_n \times 5\%)^2}$$

where A_n is area of the n th glacier. This leads to a total error of $\pm 1.13 \text{ km}^2$ in 1962 (Table 2).

The measurement accuracy of the position of the glacier front is related to sensor resolution and the co-registration error (Ye et al., 2006; Silverio and Jaquet, 2005; Hall et al., 2003; Williams et al., 1997). Once the scenes registered to the 1962 topographic base map, the uncertainty of the glacier terminus position (U_T) and areal extent (U_A) can be estimated based on the following formulas (Ye et al., 2006; Hall et al., 2003)

$$U_T = \sqrt{\sum \lambda^2} + \sqrt{\sum \varepsilon^2}$$

$$U_A = 2U_T \sqrt{\sum \lambda^2}$$

where λ is the original pixel resolution of each individual image, ε is the registration error of each individual image to the 1962 base map. Thus the calculated uncertainty of the glacier area was $\pm 0.0036 \text{ km}^2$ in 1990, and $\pm 0.0009 \text{ km}^2$ in 2006 (Table 2).

Potential errors in mapping glaciers include (1) error embedded in the method of glacier delineation, (2) error embedded in co-registration and glacier size, (3) influence of scene quality, clouds, seasonal snow and shadow (Bolch et al., 2010). The scenes were less influenced by seasonal snow and when there were few clouds. The glacier front was clear for mapping. The field investigation in 2009 found that the debris cover in Mt. Bogda was not a factor in delineating glaciers. However, there were non-ignorable errors from shadows after comparing the multitemporal imagery, including a Landsat ETM+ scene in 2009. An error of $\pm 1\%$ is estimated for the used scenes based on the tests in the study area. Hence, an error of $\pm 1\%$ was added in addition to the above estimated co-registration error. This leads to a total uncertainty of $54.79 \pm 0.561 \text{ km}^2$ for 73 investigated glaciers in the 1990 Landsat TM scene and of $112.87 \pm 1.13 \text{ km}^2$ for 191 investigated glaciers in the 2006 ASTER scene.

Table 2 The information and the estimated uncertainty of used data

Date	Data source	Resolution (m)	Accuracy RMS _{x,y} (m)	Uncertainty of terminus (m)	Uncertainty of area (km ²)
1962	Topographic map	5	<5	±12	±1.13
1990	Landsat TM	30	<30	±57	±0.0036
2006	Terra ASTER	15	<15	±31	±0.0009

2.4 Climate Conditions

Air temperature and precipitation from five national weather stations were used to quantify the peripheral climate conditions of Mt. Bogda. Basic information of these stations is shown in Table 3. Daily mean temperature and precipitation for the period 1959–2002 acquired from the National Climate Center of China Meteorological Administration, produced annual averages. These meteorological stations encircle the Mt. Bogda, which can be used to investigate the peripheral climate conditions (Fig. 1). The magnitude of the trends was derived from the slope of the regression line using the least squares method. The statistical significance of temperature and precipitation trends and the linear slopes for significant trends were determined by the Mann-Kendall test (del Río et al., 2007; Su et al., 2005).

For the southern side of Turfan and the eastern side of Qijiaojin, the MAAT in the period 1959–2002 is 14.4 and 9.7 °C

with an increasing rate of 0.042 and 0.052 °C·a⁻¹, respectively. The values are markedly greater than those of Qitai and Urumqi. However, their precipitation is only 16.3 and 37.6 mm. It is significantly less than the other stations (Table 3). Climatic settings between the northwest and southeast peripheries are quite distinct.

Those meteorological stations are all situated at low elevations (<1 200 m a.s.l.). There is no information available about the climate for high elevations. Thus, the understanding of the climatic conditions and its variations in Alpine regions is limited. However, the field measurement found that the precipitation at an altitude of 4 100 m a.s.l. is 700–750 mm in the southern slope of Mt. Bogda. It mainly occurred in the summer (Wang et al., 1989). Moreover, the data from Daxigou Station (3 539 m a.s.l.) (Fig. 2) is the unique information for understanding Alpine climate conditions of eastern Tian Shan.

Table 3 Meteorological stations used in this study and their basic information of precipitation and temperature (MAAT means annual air temperature; MAP means annual precipitation)

Station	Location	Elevation (ma.s.l.)	Parameter	<i>P</i> value	<i>R</i> value	MAAT (°C)	ΔT (°C·a ⁻¹)	MAP (mm)	ΔP (mm·a ⁻¹)
Qitai	44°01'N,	793.5	Temperature	0.015 55	0.362 67	5.2	0.025	193.1	2.48
	89°34'E		Precipitation	0.029 14	0.329 13				
Urumqi	43°47'N,	935	Temperature	0.143 79	0.224 01	7.1	0.018	262.6	4.73
	87°39'E		Precipitation	0.000 11	0.550 73				
Dabancheng	43°21'N,	1 103.5	Temperature	0.000 71	0.491 02	6.6	0.025	68.4	0.88
	88°19'E		Precipitation	0.011 98	0.375 65				
Turfan	42°56'N,	345	Temperature	<0.000 1	0.607 83	14.4	0.042	16.3	0.08
	89°12'E		Precipitation	0.874 44	0.024 52				
Qijiaojin	43°13'N,	721.4	Temperature	<0.000 1	0.606 93	9.7	0.052	37.6	-0.05
	91°44'E		Precipitation	0.803 84	-0.038 54				

3 RESULTS

3.1 Overall Changes

The distribution characteristics of 203 glaciers in 1962 were predominated by small glaciers of <1 km², which occupy 84% of the total number, and 41% of the total area. Particularly, glaciers of 0.1–0.5 km² (46%) are much more common, according to the glacier size class (<0.1, 0.1–0.5, 0.5–1.0, 1.0–2.0, 2.0–5.0, 5.0–10.0, >10.0 km²) (Fig. 3). The largest coverage in the sample is in size class 2–5 km² (31.23 km²) with 5% of the total number. The change occurring in investigated glaciers can mirror the total ice coverage of Mt. Bogda, where 469 glaciers distributed in Mt. Bogda with glaciers <1 km² accounting for 91.7% (Wang et al., 1986).

The analysis of the glacier polygon data between 1962 and 2006 yields a reduction of 21.6%, from 144.1±1.13 km² to 112.9±1.13 km². The heavy area loss suggests that Mt. Bogda is sensitive to climate warming, partly because of the great number of small glaciers. There is high variability in relative area change for small glaciers, ranging from -100% to 27%. On average, small glaciers tend to lose more of their area, while larger glaciers lose less of their area relatively. This is observed not only in this region but also in other regions (e.g., Narama et al., 2010; Paul, 2004). There is a strong tendency for glaciers smaller than 0.5 km² to disappear and 12 of these glaciers have disappeared completely. Meanwhile, 170 glaciers smaller than 1 km², accounting for 84% of the total number in sample, con-

tributed 16.3 km² to total area loss, or reduced their former area by 33%. The rest 33 glaciers reduced area by 14.9 km² with a percent change of 15.7%.

The relationship between glacier area distribution and area loss was statistically analyzed during the past several decades. Figure 4 shows that 63% of glaciers faces north (N, NE and NW). The area loss of north-facing glaciers was 17.3 km² with a percent change of -17.4%, representing 55.5% of the total glacier area loss. The south-facing (S, SE and SW) glacier reduced its area by -40.3%, and glaciers facing east and west experienced area reductions of 22.4% and 24.8%, respectively.

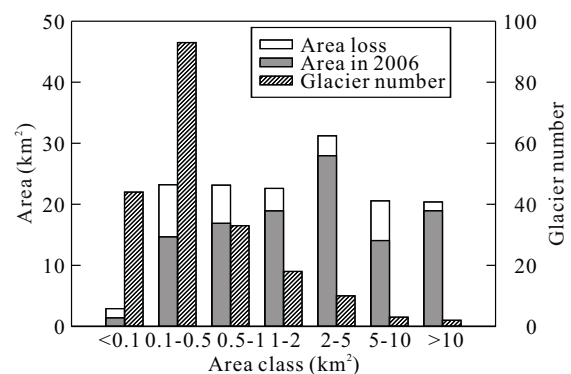


Figure 3. Glacier number, area (2006) and area loss (1962–2006) according to size class (km²: <0.1, 0.1–0.5, 0.5–1, 1–2, 2–5, 5–10, >10).

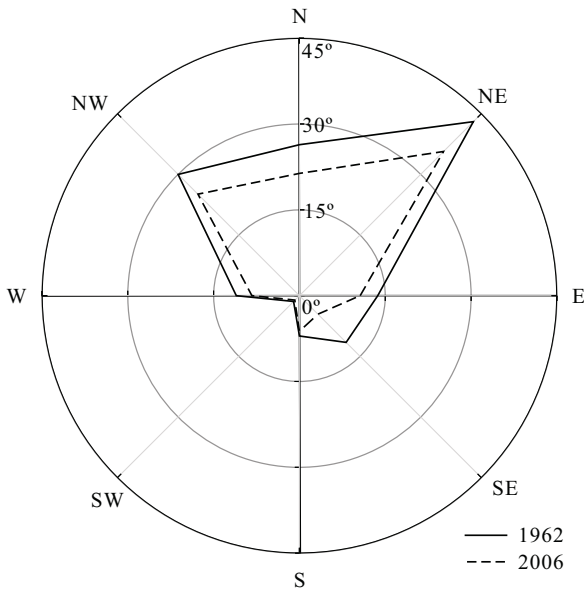


Figure 4. Aspect distribution of area loss during 1962–2006. Glaciers of Mt. Bogda tend to face north (NW, N and NE).

However, the greatest reduction was observed in the southeast sector with a rate of 60.2%.

Figure 5 shows that the strongest area loss took place for glacier terminus in an altitude of 3 600–4 000 m a.s.l. with an area reduction of 27.6 km², or 88% of total area loss. The largest relative area change occurs in altitudes ranging from 3 900–4 200 m a.s.l., where 65 glaciers with a coverage of 15.05 km² reduced by 43.6%. This section contributed 21% to total area loss. Most of the glacier terminus extends below 3 900 m a.s.l.. These parts are comprised of 169 glaciers covering 136.2 km², which accounts for 95% of the total area. Generally, large glaciers with wide altitudinal ranges extend their terminus into lower altitudes with little relative area changes, but large absolute area loss. Smaller glacier changes are significantly influenced by their topographic settings (Li et al., 2011b). A change of local climate may raise the equilibrium-line altitude of those glaciers above the maximum elevation, exposing the whole glacier to the year-round ablation zone.

The 73 glaciers in six subbasins were taken into consideration in the analysis of area and volume variations during 1962–2006. Results from a subset of the studied sample provide detailed information about glacier evolution on Mt. Bogda for the four and half decades. The area 57.45±0.73 km² in 1962

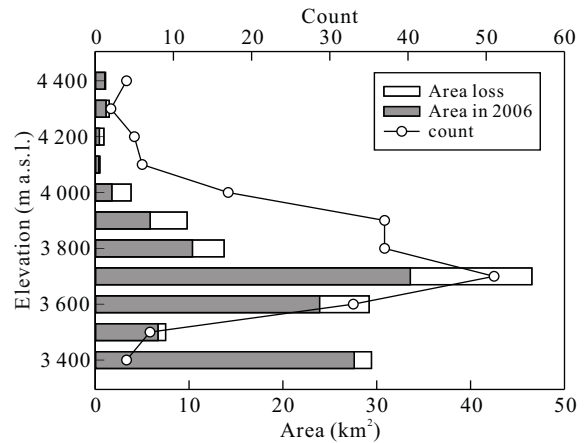


Figure 5. Distribution of glacier area with terminus elevation in 2006 (grey bars) and the area loss (white bars). The bars give values summarized in 100 m elevation intervals and the black line represents the glacier count in each of intervals.

reduced to 54.79±0.561 km² in 1990, and 48.88±0.49 km² in 2006. The relative area reduction is 4.6% during 1962–1990, while the value increased to 10.8% during the 1990–2006. The corresponding volume waste increased from 6.9% to 10.2% (Table 4). In total, the subset reduced its area and the volume was 14.9% and 16.3% during 1962 and 2006, respectively. An accelerated wastage was evident since 1990 in Mt. Bogda.

3.2 Area Change between South Side and North Side of Mt. Bogda

There are 104 glaciers in the southern slope with a mean size of 0.78 km². Their area has decreased by 25.3% of their 1962 value; meanwhile, 99 glaciers in the northern slope with an average size of 0.63 km², reduced area by 16.9% (Table 5). Due to the northern bank of the mountain being characterized by a steep and short slope, glaciers tend to be small and short in shape. The initial average length of the south and north side glacier is 1 169±12 and 1 023±12 m, and 968±31 and 863±31 m in 2006, respectively. This leads to a retreat by 201±18 and 160±18 m for the southern and northern slope glacier. It is suggested that the difference in topography may affect glacier shape and size.

Shaped by the exposure to solar radiation and the local topographic characteristics, glacier area reductions between northern and southern slopes are distinct (Fig. 6). Glacier area

Table 4 Area and volume calculated in six subbasins during 1962–1990–2006 (*A*, area, *V*, volume)

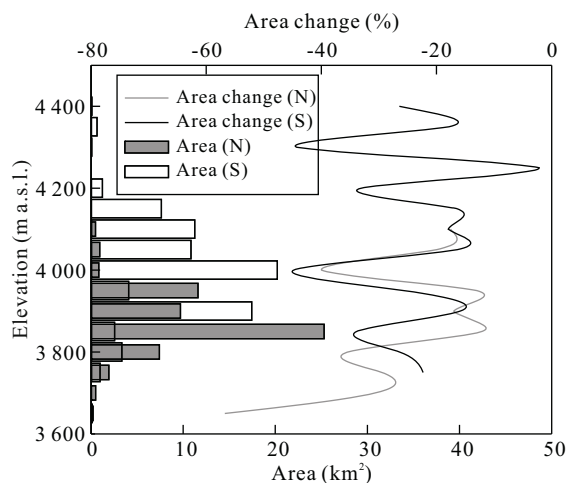
Basin	1962		1990		2006		1962–1990		1990–2006		1962–2006	
	<i>A</i> (km ²)	<i>V</i> (km ³)	<i>A</i> (km ²)	<i>V</i> (km ³)	<i>A</i> (km ²)	<i>V</i> (km ³)	<i>A</i> (%)	<i>V</i> (%)	<i>A</i> (%)	<i>V</i> (%)	<i>A</i> (%)	<i>V</i> (%)
Baiyanghe	20.91	1.243 0	19.95	1.159 1	18.95	1.103 4	-4.6	-6.7	-5.0	-4.8	-9.4	-11.2
Ganhezigou	8.35	0.471	7.62	0.408 9	6.41	0.319 2	-8.7	-13.2	-15.9	-21.9	-23.2	-32.2
Sigonghe	10.40	0.509 7	10.06	0.507 3	9.48	0.468 6	-3.3	-0.5	-5.8	-7.6	-8.8	-8.1
Sangonghe	9.49	0.340 4	9.28	0.319 8	7.83	0.289 2	-2.2	-6.1	-15.6	-9.6	-17.5	-15.0
Akesuhe	3.18	0.114 0	3.06	0.097 4	2.54	0.077 1	-3.8	-14.6	-17.0	-20.8	-20.1	-32.4
Gaoaizigou	5.12	0.189 2	4.82	0.178 2	3.69	0.141 0	-5.9	-5.8	-23.4	-20.9	-27.9	-25.5
Total	57.45	2.867 3	54.79	2.670 7	48.88	2.398 4	-4.6	-6.9	-10.8	-10.2	-14.9	-16.3

Table 5 Glacier area and number distribution in different size classes between the north and south side of Mt. Bogda

Class (km ²)	North side					South side				
	Number	Area (km ²)		Area loss		Number	Area (km ²)		Area loss	
		1962	2006	km ²	%		1962	2006	km ²	%
<0.1	25	1.73	0.87	0.86	50.0	19	1.19	0.54	0.65	54.5
0.1–0.5	46	10.40	6.76	3.64	35.0	47	12.81	7.91	4.90	38.2
0.5–1.0	14	9.20	6.37	2.83	30.8	19	13.94	10.51	3.43	24.6
1.0–2.0	6	7.23	6.41	0.82	11.3	12	15.38	12.52	2.86	18.6
2.0–5.0	6	17.78	16.20	1.58	8.9	4	13.45	11.76	1.69	12.6
5.0–10.0	1	6.30	5.96	0.34	5.4	2	14.27	8.11	6.16	43.1
>10.0	1	10.15	9.60	0.55	5.5	1	10.23	9.35	0.88	8.6
Total	99	62.79	52.16	10.63	16.9	104	81.26	60.71	20.55	25.3

Table 6 Characteristics of the glaciers investigated in detail in 2009

Glacier	GLIMS ID/CGI ID	Type	Area (km ²)	Length (km)	Aspect	H _{max} (m a.s.l.)	H _{min} (m a.s.l.)	Debris cover
Heigou No. 8	5Y813b8	Valley	5.61	7.1	SE	5 445	3 450	No
Sigonghe No. 4	5Y725d4	Cirque	2.96	3.2	W	5 445	3 660	No
Fan-shaped glacier	5Y725d5+5Y812b10	Compound	10.94	4.7	NWS	5 445	3 570	No

**Figure 6.** Glacier area distribution with elevation at 50 m intervals between the southern and northern slope; the lines represent the area change (N-northern slope; S-southern slope).

of the south side is mainly located within the altitudes of 3 900–4 100 m with covering of 63.9 km², about 79% of the total cover. Of the north side, the majority area is within the altitudes of 3 800–3 950 m with covering of 54.0 km², or 86% of the total cover. The glacier area distribution as a function of altitude shows that there is the disparity of ~100 m between both sides. The relative changes in glacier areas are synchronous between both sides.

The four visited glaciers, Heigou Glacier No. 8 (5Y813b8) on the southern slope, Sigonghe Glacier No. 4 (5Y725d4) on the northern slope, and the fan-shaped glacier (composed by glacier 5Y725d5 and 5Y812b10), provide the information regarding the accelerated trend of terminus retreat since the 1980s. These glaciers were visited in 1981 by a Chinese-Japanese combined investigation team and revisited in 2009 by the Tian Shan Glaciology Station.

Heigou Glacier No. 8 (5.6 km²) only reduced its area by

1.3% during the past 44 years. The glacier was in relatively steady retreat, and its length has been shortened from 7.4 km during the Little Ice Age to 7.1 km in 1962, and then it retreated at a rate of $-0.087 \text{ m}\cdot\text{a}^{-1}$ during 1962–1985 (Wang, 1991). By 2006, the length was 6.9 km long and the glacier retreated at a rate of $4.7 \text{ m}\cdot\text{a}^{-1}$. However, the strong surface ablation, which was observed during field investigation, may be an important character of summer melting.

Sigonghe Glacier No. 4 (3.0 km²), reduced its area by 10.6% of its 1962 size. The terminus retreated 37.0 m during 1959–1962 ($12.0 \text{ m}\cdot\text{a}^{-1}$), 113.0 m during 1962–1981 ($6.0 \text{ m}\cdot\text{a}^{-1}$) (Wu et al., 1983b), and 336.0 m during 1962–2006 ($7.6 \text{ m}\cdot\text{a}^{-1}$). The terminus retreat accelerated since the 1980s with the retreat rate changing from $6.0 \text{ m}\cdot\text{a}^{-1}$ in 1962–1981 to $8.9 \text{ m}\cdot\text{a}^{-1}$ in 1982–2006.

Fan-shaped glacier (10.2 km²), reduced its area by 7% during the period of 1962–2006. The melt water flows into the southern slope (for 5Y812b10) and northern slope (for 5Y725d5). The terminus retreated 380 m ($7.6 \text{ m}\cdot\text{a}^{-1}$) in the south subdivision and 250 m ($5 \text{ m}\cdot\text{a}^{-1}$) in the north subdivision during 1931–1981 (Wu et al., 1983b). Measured from remotely sensed data, the south and north subdivision retreated 509 m ($11.6 \text{ m}\cdot\text{a}^{-1}$) and 272 m ($6.2 \text{ m}\cdot\text{a}^{-1}$) from 1962 to 2006, respectively.

4 GLACIER DECREASING

Glaciers in Mt. Bogda experienced a net reduction in area and the size decreasing during the past four decades. Their area in each class shifts towards a smaller size class (Fig. 7a). For example, glaciers in the class of $>10.0 \text{ km}^2$ in 1962 were all shifted into the class of 5.0–10.0 km² in 2006. The phenomenon of the glacier size decrease led to area variation in different class. Their number is shifted from larger class into smaller class as well (Fig. 7b). The strong increase in count is the class of $<0.1 \text{ km}^2$.

For the purpose of understanding glacier change of different sizes, the shift analysis of the glacier number was conducted

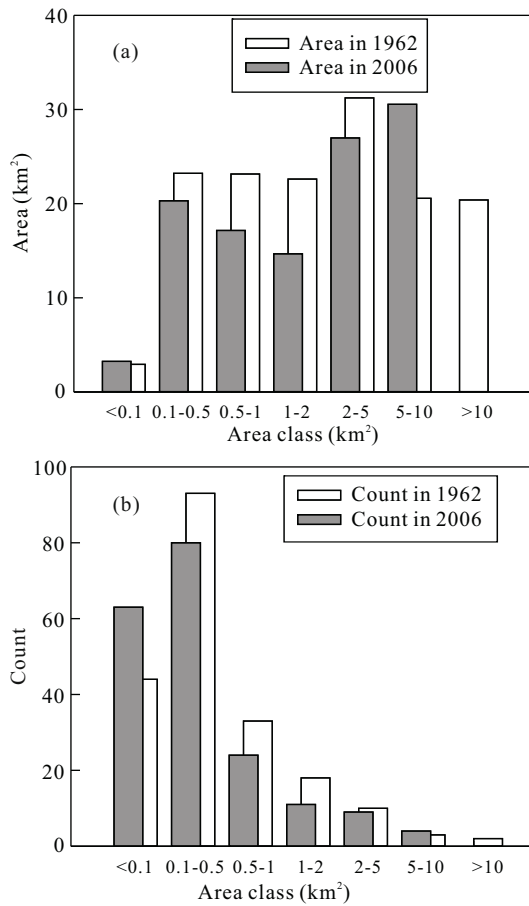


Figure 7. Glacier area (a) and number (b) markedly shifted towards the smaller class.

in detail. On condition that climate warming continued, more glaciers will decrease their size and will be in smaller classes. The individual glacier in same class differs greatly in area loss. Given that the decreased glacier shift according to class <0.1, 0.1–0.5, 0.5–1.0, 1.0–2.0, 2.0–5.0, 5.0–10.0, >10.0 km², then we denote the glacier count in the former year (1962) and recent year (2006) with NF_{0.1}, NF_{0.5}, NF₁, NF₂, NF₅, NF₁₀, NF_> and NR_{0.1}, NR_{0.5}, NR₁, NR₂, NR₅, NR₁₀, NR_>, respectively. The shifted-out glacier count from the back class into the front class n_>, n₁₀, n₅, n₂, n₁, n_{0.5}, n_{0.1} is equal to the count of shifted-in into the front class

(Table 7). The 8 vanished glaciers in the class of <0.1 km² and 4 glaciers in the class of 0.1–0.5 km² should be considered when calculating the shift number. Here we give a definition of shifted-in/out rate with n/NF to explore the extent of glacier shift in different class. There is a clear tendency that glacier in the class of 0.5–1.0 and 1.0–2.0 km² with high shifted-out rate 55% and 50%, respectively. This led more glaciers into the front class. The shifted-in rate of <0.1 km² even reach 61%. The shift process reveals that more glaciers tend to be smaller due to decreasing their size under climate warming.

5 DISCUSSION

5.1 Glacier Change

To individual glacier, topographic settings exert a marked influence on glacier changes. Thus topography should be considered a key factor in further research into the impact of climate change on glacier evolution (López-Moreno et al., 2006). These small glaciers, however, are situated at relatively high elevations, at locations sheltered from solar radiation and/or in areas with very high accumulation rates. Some glaciers have retreated into classic cirque basins tend to be stable, where they are sheltered by shadows (López-Moreno et al., 2006). Under local climatic conditions, the topographic settings may influence the glacier’s development and even their present size. Glacier facing favorable directions (N, NE and NW) loses little of their area, compared to those facing unfavorable directions (S, SE and SW). This suggests that aspect of glacier faces has an effect on its ablation.

Glacier recession of Mt. Bogda depended strongly on the size, location and climate regime at the regional scale. This is accordant with the results of Bolch and Marchenko (2009) and Bolch (2007), which arrived at an area loss of 32% by comparison between soviet glacier inventory in 1955 and Landsat ETM+ scene from 1999 in Zailiyskiy and Kungey Alatau. Research result may be effected by sample size and data source. Narama et al. (2010) suggested that the Ili-Kungöy region (Ili Alatau and Kungey Alatau) with 735 glaciers decreased in area by 12% and 4% during 1970–2000 and 2000–2007, respectively, based on Corona (1970), Landsat (2000) and ALOS (2007). The value of Bolch’s is greater than Narama’s results. The abundance of

Table 7 The process of glacier shift among area classes

Class (km ²)	<0.1	0.1–0.5	0.5–1.0	1.0–2.0	2.0–5.0	5.0–10.0	>10.0
Count in 1962	NF _{0.1}	NF _{0.5}	NF ₁	NF ₂	NF ₅	NF ₁₀	NF _{>}
	44	93	33	18	10	3	2
Count in 2006	NR _{0.1}	NR _{0.5}	NR ₁	NR ₂	NR ₅	NR ₁₀	NR _{>}
	63	80	24	11	9	4	0
Shifted count	n _{0.1}	n _{0.5}	n ₁	n ₂	n ₅	n ₁₀	n _{>}
Shifted-out	8 ⁽⁷⁾	27 ⁽⁶⁾	18 ⁽⁵⁾	9 ⁽⁴⁾	2 ⁽³⁾	1 ⁽²⁾	2 ⁽¹⁾
Shifted-in	27	18	9	2	1	2	
Shifted-out rate (%)	18	29	55	50	20	33	100
Shifted-in rate (%)	61	19	27	11	10	67	

Note: ⁽¹⁾ NF_>-NR_>; ⁽²⁾ NF₁₀+(1)-NR₁₀; ⁽³⁾ NF₅+(2)-NR₅; ⁽⁴⁾ NF₂+(3)-NR₂; ⁽⁵⁾ NF₁+(4)-NR₁; ⁽⁶⁾ NF_{0.5}+(5)-NR_{0.5} -4; ⁽⁷⁾ NF_{0.1}+(6)-NR_{0.1}.

glaciers in different size classes has a strong effect on the total glacier area loss (Narama et al., 2010). This is one of the reasons for the above differences. It is suggested that the size distribution difference can lead to distinct change of glacier relative area between regions. Though local climatic conditions or micro-climatic factors were major factors resulting in different responses to climatic warming, the glacier retreat in Tian Shan is beyond question. Glaciers in Mt. Kalik, located in the eastern-most of Tian Shan, have reduced their area by 5.3% during 1971/72–2001/02 (Wang et al., 2009). Taking into account the glacier change in Mt. Bogda, the strong reduction in glacier area and extreme water shortage in the Turfan-Hami Basin may become an increasing threat to this region in the future.

Glacier area shrinkage is generally accompanied by volume wastage. For assessing glacier wastage, the ice loss can be estimated by repeated DEMs (Paul and Haeberli, 2008; Larsen et al., 2007; Stearns and Hamilton, 2007). The impact of ice loss on future runoff can also be predicted by the HBV-model together with climatic scenarios (Hagg et al., 2007). On the condition of more abundant surface area data, a common and simple way to estimate glacier volume is to estimate the scaling relationship between glacier volume and area (Liu et al., 2003; Bahr et al., 1997). A detailed analysis of scaling methods in deriving future volume evolution suggests that volume calculations are highly sensitive to the choice of the scaling constants (Radić et al., 2008). Accurate estimation of glacier volume is limited by methods or data. Since there is no available mass balance or ice thickness information for detailed investigation on Mt. Bogda, a subset of glacier was selected in the sample to reveal the trend of glacier area shrinkage and the level of volume loss during the past four decades. The results suggest that glacier area shrinkage has accelerated since 1990s, together with the area and volume reduction changed from 4.6% and 6.9% during 1962–1990 into 10.8% and 10.2% during 1990–2006, respectively.

5.2 Climate Change

Several analyses show that climate factors, such as increased temperature and decreased precipitation, are two key factors responsible for glacier retreat (Kaser, 1999; Wagon et al., 1999). The analysis shows that air temperature tends to increase in this region. However, it should be stressed that due to a lack of available climate data at high altitudes, the statistical analysis depends on the surrounding lowland stations. The presented analysis suggest that the air temperature increases in a similar trend when being compared to the Daxigou Climate Station (43°06'N, 86°50'E, 3 539 m a.s.l., about 2 km down-

stream of the UG1). The UG1 is in a continued negative mass balance since 1959, and the mass loss is mainly controlled by summer temperatures (Ye et al., 2005). Successful evaluation of the climatic controls on glaciers may require special in-situ studies of mass balance, or data in spatio-temporal meteorological variability. The understanding of the melting process needs energy balance models and temperature-index models. Many studies have revealed a high correlation between glacier melt and air temperature. Braithwaite and Olesen (1989) found a correlation coefficient of 0.96 between annual ice ablation and positive air temperature sums. The information provided by weather stations show an increase of the mean annual air temperature ranging from 0.018–0.052 °C·a⁻¹ and an increased rate of 0.08–4.73 mm·a⁻¹ (except in Qijiaojin) for precipitation (Table 3). The regional climate warming enhanced the glacier melt, as well as the increased runoff. According to investigation in UG1 (Ye et al., 2005), the effect of climate warming overcomes the effect of increased precipitation on glacier mass balance and leads to higher ablation.

Further analysis of meteorological data around Mt. Bogda shows that summer air temperatures (June–August; JJA) remained around the same level during the period of 1959–2002, while winter air temperatures (October–December; OND) increased significantly during 1991–2002 (Table 8). Although ice-melting is mainly controlled by summer air temperatures; the overall increase in winter air temperatures reduced the cold-storage ability of the ice body. Moreover, the extended ablation period, especially for Turfan and Qijiaojin, created an optimal environment for glacier melting. In Turfan and Qijiaojin, the average number of days >0 °C in the 1991–2002 period extended 12 days in comparison with 1959–1990. The north and western periphery were also featured by increased summer precipitation (~20 mm). The highly concentrated summer precipitation leads to high sensitivity of the glacier mass balance to climate change (Fujita, 2008).

The significant increase in air temperature since 1990 was found in five investigation stations, while the precipitation increase only occurred in Qitai and Urumqi stations (Table 3). Temperature and precipitation changes in the northern side of Mt. Bogda reported here seem to conform to a regime shift from a warm-dry to warm-wet pattern over Northwest China (Shi et al., 2006, 2003). However, the obviously increased precipitation in the north side and slightly increased precipitation in the south side could not keep the glacier from retreating and thinning under the warmer climate. It is suggested that the enhanced summer precipitation could not counteract the effect of warming.

Table 8 Meteorological stations and climate data used in this study (tem.-temperature; pre.-precipitation)

Station	Days of >0 °C		JJA tem. (°C)		OND tem. (°C)		JJA pre. 1959–1990		JJA pre. 1990–2002	
	1959–1990	1991–2002	1959–1990	1991–2002	1959–1990	1991–2002	(mm)	(%)	(mm)	(%)
Qitai	229	233	20.1	19.9	-4.1	-3.5	71.9	38	91.1	43
Urumqi	236	237	21.6	21.0	-2.0	-0.8	72.1	31	93.6	32
Dabancheng	236	240	18.6	18.7	-1.3	-0.6	42.1	70	72.6	81
Turfan	278	290	28.6	28.7	2.8	4.2	7.3	47	6.8	43
Qijiaojin	250	262	23.2	24.4	-0.1	1.4	26.6	74	24.4	74

The increase of air temperature was observed in the Tian Shan Alpine areas (Aizen et al., 1997), and the glacier area was in a definite trend of recession in Ala Archa and Akshirak over the last 150 years. Especially since the 1970s, glacier recession experienced an acceleration resulting from abrupt climate change (Aizen et al., 2007). Bolch (2007) suggested that the glacier retreat in northern Tian Shan (Kazakhstan/Kyrgyzstan) is dependent not only on the size, but also on the climate regime. Glacier retreat correlates well with increased air temperature, which was mainly due to a temperature increase in autumn and winter. The most pronounced rise in annual temperature in central Asia has been reported by Giese et al. (2007) and Aizen et al. (1997). Noticeable climate warming has been taking place in central Asia over the last half century. The long-term observed UGI can be used to understand their changes on Mt. Bogda glaciers. With climatic warming, the remarkable changes have occurred on the UGI, including glacial zone, glacial temperature, glacier outline, and with area reduction by 14% during 1962–2006 (Li et al., 2007). Its strong negative mass balance is governed by summer air temperature (Wang et al., 2014; Ye et al., 2005).

An acceleration of the retreat of Mt. Bogda glaciers occurred in 1990–2006 in comparison with 1962–2006 (Table 5). This result is in accordance with the climate change (Table 8). Glacier retreat was mainly affected by change of air temperature and precipitation. The precipitation increase partly offset by the increasing proportion of liquid precipitation in the main accumulation months (JJA), and partly increase in precipitation is required to offset the effects of warming on glacier mass balance. Moreover, small glacier in this studied area exhibits higher sensitivity to temperature changes leading to a strong shrinkage.

6 CONCLUSIONS

Mt. Bogda glacier experienced heavy area loss during the period of 1962–2006. The area was reduced by 21.6%, and 12 glaciers vanished completely. Large quantity of small glaciers was responsible for this heavy reduction. The small glaciers (<1 km²), accounted for 84% in number, contributed 52% of the total area loss. Glaciers in 0.5–2.0 km² lose more of their area and tend to small. The wide gap of area reduction between the southern and northern slopes is visible, for 25% and 17%, respectively. The climate settings are characterized by observed warming in the winter and an extended ablation period, providing a favorable force for glacier melting.

Strong area reduction must be accompanied by heavy ice loss. Large glacier produces great quantities of glacier water when melting. Strong ice wastage will threaten potential hydrological regimes and local communities in a long run. The vanished Karez of Turfan Basin is closely related to climate warming and runoff decrease induced by glacier shrinkage.

ACKNOWLEDGMENTS

This study was supported by the Initial Funding of Doctor Scientific Research (No. LZCU-BS2013-06), the Project of Humanities and Social Sciences from the Ministry of Education of China (No. 13YJC790009), the National Basic Research Program of China (No. 2013CBA01801), the National Natural

Science Foundation of China (No. 41471058) and the Funds for the Creative Research Groups of China (No. 41121001). We also thank those colleagues who worked on glacial observations at the Tian Shan Glaciology Station and who provided the field data for this study. The final publication is available at Springer via <http://dx.doi.org/10.1007/s12583-016-0614-7>.

REFERENCES CITED

- Aizen, V. B., Aizen, E. M., Melack, J. M., et al., 1997. Climatic and Hydrologic Changes in the Tien Shan, Central Asia. *Journal of Climate*, 10(6): 1393–1404. doi:10.1175/1520-0442(1997)010<1393:cahcit>2.0.co;2
- Aizen, V. B., Kuzmichenok, V. A., Surazakov, A. B., et al., 2007. Glacier Changes in the Tien Shan as Determined from Topographic and Remotely Sensed Data. *Global and Planetary Change*, 56(3/4): 328–340. doi:10.1016/j.gloplacha.2006.07.016
- Bahr, D. B., Meier, M. F., Peckham, S. D., 1997. The Physical Basis of Glacier Volume-Area Scaling. *Journal of Geophysical Research*, 102(B9): 20355–20362. doi:10.1029/97jb01696
- Bahr, D. B., Dyurgerov, M., Meier, M. F., 2009. Sea-Level Rise from Glaciers and Ice Caps: A Lower Bound. *Geophysical Research Letters*, 36(3): L03501. doi:10.1029/2008gl036309
- Böhner, J., 2006. General Climatic Controls and Topoclimatic Variations in Central and High Asia. *Boreas*, 35(2): 279–295. doi:10.1111/j.1502-3885.2006.tb01158.x
- Bolch, T., 2007. Climate Change and Glacier Retreat in Northern Tien Shan (Kazakhstan/Kyrgyzstan) Using Remote Sensing Data. *Global and Planetary Change*, 56(1/2): 1–12. doi:10.1016/j.gloplacha.2006.07.009
- Bolch, T., Buchroithner, M., Pieczonka, T., et al., 2008. Planimetric and Volumetric Glacier Changes in the Khumbu Himal, Nepal, since 1962 Using Corona, Landsat TM and ASTER Data. *Journal of Glaciology*, 54(187): 592–600. doi:10.3189/002214308786570782
- Bolch, T., Marchenko, S., 2009. Significance of Glaciers, Rockglaciers and Ice-Rich Permafrost in the Northern Tien Shan as Water Towers under Climate Change Conditions. *Proceedings of the Workshop Assessment of Snow-Glacier and Water Resources in Asia*, 2006: 28–30
- Bolch, T., Menounos, B., Wheate, R., 2010. Landsat-Based Inventory of Glaciers in Western Canada, 1985–2005. *Remote Sensing of Environment*, 114(1): 127–137. doi:10.1016/j.rse.2009.08.015
- Braithwaite, R. J., Olesen, O. B., 1989. Calculation of Glacier Ablation from Air Temperature, West Greenland. *Glaciology and Quaternary Geology*, 19: 219–233. doi:10.1007/978-94-015-7823-3_15
- Chen, J. M., Liu, C. H., Jin, M. X., 1996. Application of the Repeated Aerial Photogrammetry to Monitoring Glacier Variation in the Drainage Area of the Urumqi River. *Journal of Glaciology and Geocryology*, 18(4): 331–336 (in Chinese with English Abstract)
- Cubasch, U., Meehl, G., 2001. Projections of Future Climate Change, Climate Change 2001: The Scientific Basis. IPCC 2001 Report, Cambridge. 525–582
- del Rio, S., Fraile, R., Herrero, L., et al., 2007. Analysis of

- Recent Trends in Mean Maximum and Minimum Temperatures in a Region of the NW of Spain (Castilla y León). *Theoretical and Applied Climatology*, 90(1/2): 1–12. doi:10.1007/s00704-006-0278-9
- Drieger, C. L., Kennard, P. M., 1986. Glacier Volume Estimation on Cascade Volcanoes: An Analysis and Comparison with Other Methods. *Annals of Glaciology*, 8: 59–64
- Fujita, K., 2008. Effect of Precipitation Seasonality on Climatic Sensitivity of Glacier Mass Balance. *Earth and Planetary Science Letters*, 276(1/2): 14–19. doi:10.1016/j.epsl.2008.08.028
- Fang, S. F., Pei, H., Liu, Z. H., et al., 2010. Water Resources Assessment and Regional Virtual Water Potential in the Turpan Basin, China. *Water Resources Management*, 24(13): 3321–3332. doi:10.1007/s11269-010-9608-x
- Farinotti, D., Huss, M., Bauder, A., et al., 2009. A Method to Estimate the Ice Volume and Ice-Thickness Distribution of Alpine Glaciers. *Journal of Glaciology*, 55(191): 422–430. doi:10.3189/002214309788816759
- Giese, E., Mossig, I., Rybski, D., et al., 2007. Long-Term Analysis of Air Temperature Trends in Central Asia. *Erdkunde*, 61(2): 186–202. doi:10.3112/erdkunde.2007.02.05
- Haerberli, W., Hoelzle, M., 1995. Application of Inventory Data for Estimating Characteristics and Regional Climate-Change Effects on Mountain Glaciers: A Pilot Study with the European Alps. *Annals of Glaciology*, 21: 206–212
- Hagg, W., Braun, L. N., Kuhn, M., et al., 2007. Modelling of Hydrological Response to Climate Change in Glacierized Central Asian Catchments. *Journal of Hydrology*, 332(1/2): 40–53. doi:10.1016/j.jhydrol.2006.06.021
- Hall, D. K., Bayr, K. J., Schöner, W., et al., 2003. Consideration of the Errors Inherent in Mapping Historical Glacier Positions in Austria from the Ground and Space (1893–2001). *Remote Sensing of Environment*, 86(4): 566–577. doi:10.1016/s0034-4257(03)00134-2
- Jin, R., Li, X., Che, T., et al., 2005. Glacier Area Changes in the Pumqu River Basin, Tibetan Plateau, between the 1970s and 2001. *Journal of Glaciology*, 51(175): 607–610. doi:10.3189/172756505781829061
- Kääb, A., Huggel, C., Paul, F., et al., 2002. Glacier Monitoring from ASTER Imagery: Accuracy and Application. *Proceedings of EARSeL*, 2(1): 43–53
- Kaser, G., 1999. A Review of the Modern Fluctuations of Tropical Glaciers. *Global and Planetary Change*, 22(1–4): 93–103. doi:10.1016/s0921-8181(99)00028-4
- Khromova, T. E., 2003. Late-Twentieth Century Changes in Glacier Extent in the Ak-Shirak Range, Central Asia, Determined from Historical Data and ASTER Imagery. *Geophysical Research Letters*, 30(16): 1863. doi:10.1029/2003gl017233
- Kutuzov, S., Shahgedanova, M., 2009. Glacier Retreat and Climatic Variability in the Eastern Terskey-Alatoo, Inner Tien Shan between the Middle of the 19th Century and Beginning of the 21st Century. *Global and Planetary Change*, 69(1/2): 59–70. doi:10.1016/j.gloplacha.2009.07.001
- Larsen, C. F., Motyka, R. J., Arendt, A. A., et al., 2007. Glacier Changes in Southeast Alaska and Northwest British Columbia and Contribution to Sea Level Rise. *Journal of Geophysical Research*, 112(F1): F01007. doi:10.1029/2006jf000586
- Li, B. L., Zhu, A. X., Zhang, Y. C., et al., 2006. Glacier Change over the Past Four Decades in the Middle Chinese Tien Shan. *Journal of Glaciology*, 52(178): 425–432. doi:10.3189/172756506781828557
- Li, K. M., Li, Z. Q., Gao, W. Y., et al., 2011a. Recent Glacial Retreat and Its Effect on Water Resources in Eastern Xinjiang. *Chinese Science Bulletin*, 56(33): 3596–3604. doi:10.1007/s11434-011-4720-8
- Li, K. M., Li, H. L., Wang, L., et al., 2011b. On the Relationship between Local Topography and Small Glacier Change under Climatic Warming on Mt. Bogda, Eastern Tian Shan, China. *Journal of Earth Science*, 22(4): 515–527. doi:10.1007/s12583-011-0204-7
- Li, Z. Q., Han, T. D., Jin, Z. F., et al., 2003. A Summary of 40-Year Observed Variation Fact of Climate and Glacier No. 1 at Headwater of Urumqi River, Tianshan, China. *Journal of Glaciology and Geocryology*, 25(2): 117–123 (in Chinese with English Abstract)
- Li, Z. Q., Shen, Y. P., Wang, F. T., et al., 2007. Response of Glacier Melting to Climate Change—Take Urumqi Glacier No. 1 as an Example. *Journal of Glaciology and Geocryology*, 29(3): 333–342 (in Chinese with English Abstract)
- Linsbauer, A., Paul, F., Hoelzle, M., et al., 2009. The Swiss Alps without Glaciers—AGIS-Based Modeling Approach for Reconstruction of Glacier Beds. *Proceedings of Geomorphometry*, 31: 243–247
- Liu, S. Y., Sun, W. X., Shen, Y. P., et al., 2003. Glacier Changes since the Little Ice Age Maximum in the Western Qilian Shan, Northwest China, and Consequences of Glacier Runoff for Water Supply. *Journal of Glaciology*, 49(164): 117–124. doi:10.3189/172756503781830926
- Liu, S. Y., Ding, Y. J., Shangguan, D. H., et al., 2006. Glacier Retreat as a Result of Climate Warming and Increased Precipitation in the Tarim River Basin, Northwest China. *Annals of Glaciology*, 43(1): 91–96. doi:10.3189/172756406781812168
- López-Moreno, J. I., Nogués-Bravo, D., Chueca-Cía, J., et al., 2006. Change of Topographic Control on the Extent of Cirque Glaciers since the Little Ice Age. *Geophysical Research Letters*, 33(24): L24505. doi:10.1029/2006gl028204
- Niederer, P., Bilenko, V., Ershova, N., et al., 2007. Tracing Glacier Wastage in the Northern Tien Shan (Kyrgyzstan/Central Asia) over the Last 40 Years. *Climatic Change*, 86(1/2): 227–234. doi:10.1007/s10584-007-9288-6
- Narama, C., Shimamura, Y., Nakayama, D., et al., 2006. Recent Changes of Glacier Coverage in the Western Terskey-Alatoo Range, Kyrgyz Republic, Using Corona and Landsat. *Annals of Glaciology*, 43(1): 223–229. doi:10.3189/172756406781812195
- Narama, C., Kääb, A., Duishonakunov, M., et al., 2010. Spatial Variability of Recent Glacier Area Changes in the Tien Shan Mountains, Central Asia, Using Corona (~1970), Landsat (~2000), and ALOS (~2007) Satellite Data. *Global and Planetary Change*, 71(1/2): 42–54. doi:10.1016/j.gloplacha.2009.08.002
- Paul, F., 2004. Rapid Disintegration of Alpine Glaciers Ob-

- served with Satellite Data. *Geophysical Research Letters*, 31(21): L21402. doi:10.1029/2004gl020816
- Paul, F., Andreassen, L. M., 2009. A New Glacier Inventory for the Svartisen Region, Norway, from Landsat ETM+ Data: Challenges and Change Assessment. *Journal of Glaciology*, 55(192): 607–618. doi:10.3189/002214309789471003
- Paul, F., Haeberli, W., 2008. Spatial Variability of Glacier Elevation Changes in the Swiss Alps Obtained from Two Digital Elevation Models. *Geophysical Research Letters*, 35(21): L21502. doi:10.1029/2008gl034718
- Racoviteanu, A. E., Paul, F., Raup, B., et al., 2009. Challenges and Recommendations in Mapping of Glacier Parameters from Space: Results of the 2008 Global Land Ice Measurements from Space (GLIMS) Workshop, Boulder, Colorado, USA. *Annals of Glaciology*, 50(53): 53–69. doi:10.3189/172756410790595804
- Radić, V., Hock, R., Oerlemans, J., 2008. Analysis of Scaling Methods in Deriving Future Volume Evolutions of Valley Glaciers. *Journal of Glaciology*, 54(187): 601–612. doi:10.3189/002214308786570809
- Raup, B., Kääb, A., Kargel, J. S., et al., 2007a. Remote Sensing and GIS Technology in the Global Land Ice Measurements from Space (GLIMS) Project. *Computers & Geosciences*, 33(1): 104–125. doi:10.1016/j.cageo.2006.05.015
- Raup, B., Racoviteanu, A., Khalsa, S. J. S., et al., 2007b. The GLIMS Geospatial Glacier Database: A New Tool for Studying Glacier Change. *Global and Planetary Change*, 56(1/2): 101–110. doi:10.1016/j.gloplacha.2006.07.018
- Shi, Y. F., Shen, Y. P., Li, D., et al., 2003. Discussion on the Present Climate Change from Warm-Dry to Warm-Wet in Northwest China. *Quaternary Sciences*, 23(2): 152–164
- Shi, Y. F., Shen, Y. P., Kang, E. S., et al., 2006. Recent and Future Climate Change in Northwest China. *Climatic Change*, 80(3/4): 379–393. doi:10.1007/s10584-006-9121-7
- Silverio, W., Jaquet, J. M., 2005. Glacial Cover Mapping (1987–1996) of the Cordillera Blanca (Peru) Using Satellite Imagery. *Remote Sensing of Environment*, 95(3): 342–350. doi:10.1016/j.rse.2004.12.012
- Stearns, L. A., Hamilton, G. S., 2007. Rapid Volume Loss from Two East Greenland Outlet Glaciers Quantified Using Repeat Stereo Satellite Imagery. *Geophysical Research Letters*, 34(5): L05503. doi:10.1029/2006gl028982
- Su, B. D., Jiang, T., Jin, W. B., 2005. Recent Trends in Observed Temperature and Precipitation Extremes in the Yangtze River Basin, China. *Theoretical and Applied Climatology*, 83(1–4): 139–151. doi:10.1007/s00704-005-0139-y
- Svoboda, F., Paul, F., 2009. A New Glacier Inventory on Southern Baffin Island, Canada, from ASTER Data: I. Applied Methods, Challenges and Solutions. *Annals of Glaciology*, 50(53): 11–21. doi:10.3189/172756410790595912
- Wang, S. J., Du, J. K., He, Y. Q., 2014. Spatial-Temporal Characteristics of a Temperate-Glacier's Active-Layer Temperature and Its Responses to Climate Change: A Case Study of Baishui Glacier No. 1, Southeastern Tibetan Plateau. *Journal of Earth Science*, 25(4): 727–734. doi:10.1007/s12583-014-0460-4
- Wang, Y., Qiu, J., 1983. Distributive Features of the Glaciers in Bogda Region, Tian Shan. *Journal of Glaciology and Geocryology*, 5(3): 17–24 (in Chinese with English Abstract)
- Wang, Y., Liu, C., Ding, L., et al., 1986. Glacier Inventory of China (III): Tian Shan Mountains (Interior Drainage Area of Scattered Flow in East). Science Press, Beijing (in Chinese)
- Wang, Z., Shao, W., Zhang, J., et al., 1989. The Observed and Calculation of Rainfall at the Zone with High Elevation on the South Slope of the Bogda-Peak Region. In: Shi, Y., Qu, Y., eds., *Water Resource and Environment in Caiwopu-Dabancheng Region*. Science Press, Beijing
- Wang, Z., 1991. A Discussion on the Questions of Development of Heigou Glacier No. 8, Bogda-Peak Region. *Journal of Glaciology and Geocryology*, 13(2): 141–146 (in Chinese with English Abstract)
- Wang, Y. T., Hou, S. G., Liu, Y. P., 2009. Glacier Changes in the Karlik Shan, Eastern Tien Shan, during 1971/72–2001/02. *Annals of Glaciology*, 50(53): 39–45. doi:10.3189/172756410790595877
- Wagnon, P., Ribstein, P., Kaser, G., et al., 1999. Energy Balance and Runoff Seasonality of a Bolivian Glacier. *Global and Planetary Change*, 22(1–4): 49–58. doi:10.1016/s0921-8181(99)00025-9
- Williams, R. S., Hall, D. K., Chien, J. Y. L., 1997. Comparison of Satellite-Derived with Ground-Based Measurements of the Fluctuations of the Margins of Vatnajökull, Iceland, 1973–92. *Annals of Glaciology*, 24: 72–80
- WGMS, 2008. Global Glacier Changes: Facts and Figure. In: Zemp, M., Roer, I., Kääb, A., et al., eds., *United Nations Environment Programme. World Glacier Monitoring Service*, Zürich
- Wu, G., Yutaka, A., Qiu, J., 1983a. Physical Geographic Features and Climatic Conditions of Glacial Development in Bogda Area, Tian Shan. *Journal of Glaciology and Geocryology*, 5(3): 5–16 (in Chinese with English Abstract)
- Wu, G., Zhang, S., Wang, Z., 1983b. Retreat and Advance of Modern Glaciers in Bogda, Tian Shan. *Journal of Glaciology and Geocryology*, 5(3): 143–152 (in Chinese with English Abstract)
- Xie, Z., Wu, G., Wang, Z., et al., 1983. Ice Formation of Glaciers on the Northern Slope of Bogda, Tian Shan. *Journal of Glaciology and Geocryology*, 5(3): 37–44 (in Chinese with English Abstract)
- Ye, B. S., Yang, D. Q., Jiao, K. Q., et al., 2005. The Urumqi River Source Glacier No. 1, Tianshan, China: Changes over the Past 45 Years. *Geophysical Research Letters*, 32(21): L21504. doi:10.1029/2005gl024178
- Ye, Q. H., Kang, S. C., Chen, F., et al., 2006. Monitoring Glacier Variations on Geladandong Mountain, Central Tibetan Plateau, from 1969 to 2002 Using Remote-Sensing and GIS Technologies. *Journal of Glaciology*, 52(179): 537–545. doi:10.3189/172756506781828359